Dynamic Scaling of Bred Vectors in Chaotic Extended Systems

Cristina Primo,[1,2,3] Miguel A. Rodríguez,[1] Juan M. López,[1] and Ivan Szendro[1,4]

[1] *Instituto de Física de Cantabria (CSIC–UC), E-39005 Santander, Spain*
[2] *Instituto Nacional de Meteorología CMT/CAS, Santander, Spain*
[3] *Departamento de Matemática Aplicada, Universidad de Cantabria, Avda. Los Castros, E-39005 Santander, Spain*
[4] *Departamento de Física Moderna, Universidad de Cantabria, Avda. Los Castros, E-39005 Santander, Spain*

(Dated: February 8, 2008)

We argue that the spatiotemporal dynamics of bred vectors in chaotic extended systems are related to a kinetic roughening process in the Kardar-Parisi-Zhang universality class. This implies that there exists a characteristic length scale corresponding to the typical extend over which the finite-size perturbation is actually correlated in space. This can be used as a quantitative parameter to characterize the degree of projection of the bred vectors into the dynamical attractor.

PACS numbers: 05.45.Jn, 05.45.Ra, 05.40.-a

A standard tool for studying chaotic behavior in dynamical systems is the computation of the characteristic Lyapunov exponents, which, roughly speaking, measure the typical exponential growth rate of an infinitesimal disturbance [1, 2]. The characteristic Lyapunov exponents in extended systems are defined in a similar way as their low-dimensional counterpart and can be calculated from the linearization of the equations of motion [3, 4]. The main point is that the growth of an infinitesimal perturbation is described by the linear equations for the tangent space, the so-called Lyapunov vectors. However, for many practical purposes, Lyapunov vectors may be irrelevant as indicators of, for instance, the predictability time. Indeed, in realistic situations, the error in the initial condition is finite. The important fact is that the evolution of finite errors is not confined to the tangent space, as defined by the growth of linearized perturbations, but is controlled by the complete non-linear dynamics. In order to deal with realistic perturbations, the concept of finite size Lyapunov exponents has been found [5] to be useful to analyze predictability in high-dimensional systems [3].

A good example with important practical application occurs in weather forecasting research, where one deals with the whole Earth's atmosphere– an extremely high dimensional system in which initial conditions can be determined only with limited accuracy. In this context, Patil *et. al.* have recently introduced the concept of *bred vector* (BV) [6, 7], as the spatio-temporal evolution of a statistical ensemble of non-infinitesimal perturbations. From the analysis of real data provided by the US National Weather Service, Patil *et. al.* have proposed and measured an effective local finite-time dimension, by means of the so-called local BV dimension statistic [6, 7]. Regions of low BV dimension are identified as more predictable than locations where dimension is high. The method has recently been applied to 2D coupled map lattices in which nonlinear time series analysis has been used to make local predictions of trajectories at low dimension sites [8]. Breeding techniques constitute an important tool in modern weather forecasting research [7] and one can envisage that BVs can be used in other spatially extended systems with chaotic dynamics where local short time forecasts can also be feasible [8]. However, many questions concerning statistical and dynamical properties of BVs are still unanswered. The aim of this Letter is to shed some light into these questions.

In this Letter we study the spatiotemporal dynamics of homogeneous finite-size errors and focuss on the propagation dynamics of BVs in chaotic extended systems. We argue that, after a suitable transformation of variables, the BV dynamics can be interpreted as a kinetic roughening process in the Kardar-Parisi-Zhang universality class [9]. We also find that the breeding procedure introduces a characteristic length scale corresponding to the typical extend over which the finite-size perturbation is actually correlated in space. This can be used as a quantitative parameter to characterize the degree of projection of the BVs into the dynamical attractor, which is of major interest in probabilistic forecasting techniques based on ensembles of BVs.

We exemplify our results by means of numerical simulations of coupled map lattices in one dimension, which are simple model systems exhibiting space-time chaos and convenient as far as the computing time is concerned. Then, we shall be considering a coupled map array consisting of L chaotic oscillators given by

$$u(x,t+1) = \nu\, f(u(x+1,t)) + \nu\, f(u(x-1,t)) + (1-2\,\nu)\, f(u(x,t)) \qquad (1)$$

where $x = 1, 2, \ldots, L$, $f(u)$ is a chaotic map, ν is the coupling constant, and periodic boundary conditions are imposed. We have fixed the coupling to $\nu = 1/3$ in all the simulations presented in this Letter. We have carried out simulations for two different choices of the map, the chaotic logistic map $f(u) = 4u(1-u)$, $0 \le u \le 1$ and the tent map $f(u) = 1 - 2|u - 1/2|$, $0 \le u \le 1$. For the sake of brevity, all the results we present below correspond to coupled logistic maps, but similar results were obtained for the tent map.

Scaling of finite perturbations.– Let us first consider the evolution of finite size homogeneously perturbed trajectories in our model system (1). Given an initial condition $u^0(x,0)$, the solution $u^0(x,t)$ is univocally determined by computing Eq.(1) for a number

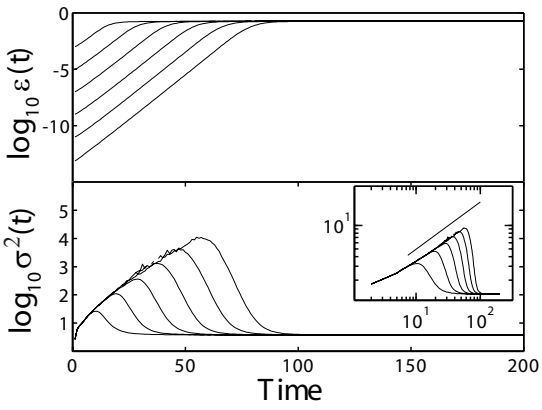

FIG. 1: Numerical results for the propagation of finite-size errors in the coupled logistic maps. Upper panel shows the amplitude factor $\epsilon(t)$ *vs.* time for perturbations starting with initial amplitudes of $\epsilon_0 = 10^{-3}, 10^{-5}, 10^{-7}, 10^{-9}, 10^{-11}$ and 10^{-13} (from top to bottom) in 1D lattices of $L = 1024$ sites and results were averaged over 600 different initial conditions. Lower panel shows the variance $\sigma^2(t)$ for the same initial perturbations as before and ϵ_0 decreasing from top to bottom. The same data are plotted in log-log scale in the inset to show the power-law behavior $\sigma^2(t) \sim t^{2\beta}$. The straight line has a slope 0.60 and is plotted to guide the eye.

t of time steps. This will be our reference trajectory and we shall be studying the evolution of finite perturbations around that reference solution. Since we are interested here in the propagation of real (non-infinitesimal) errors, we should avoid linearization of Eq.(1). Instead, we compute the trajectories generated by iterating (1) for an ensemble of initial conditions $u(x,0) = u^0(x,0) + \delta u(x,0)$, where $\delta u(x,0)$ is uniformly distributed in $(-\epsilon_0, \epsilon_0)$. For each iteration of the lattice (1) the difference $\delta u(x,t) = u(x,t) - u^0(x,t)$ between the reference trajectory and every one of the disturbed solutions is calculated and represents the evolution of homogeneously distributed finite errors in the system. Although the disturbances are initially homogeneous and uncorrelated in space, as time goes by, they propagate, get correlated, and grow exponentially in size. The statistical fluctuations of disturbances can be characterized by studying now the ensemble of finite perturbations $\{\delta u_n(x,t)\}_{n=1}^N$, which correspond to N independent realizations of the initial perturbation. In our simple model we can use ensembles of hundred of samples to obtain a good statistics.

Firstly, we introduce what we call the *amplitude factor* $\epsilon(t)$ as the spatial geometrical mean value of the perturbation:

$$\epsilon(t) \equiv \prod_{x=1}^{L} |\delta u(x,t)|^{1/L}, \tag{2}$$

which, as we shall see below, contains the information about the dominant exponential growth rate. In Fig. 1 we plot $\log \epsilon(t)$ *vs.* time for different values of the initial perturbation amplitude ϵ_0. We can see that for times $t < t_{\rm lin}(\epsilon_0)$ the average amplitude factor grows exponentially in time $\epsilon(t) \approx \epsilon_0 \exp(\lambda t)$. We demonstrate below that λ indeed corresponds to the maximal Lyapunov exponent. For longer times, $t > t_{\rm lin}(\epsilon_0)$ the amplitude factor saturates to a constant value. Both, the saturation constant and the maximal Lyapunov exponent, are independent of the initial perturbation size ϵ_0. However, the saturation times $t_{\rm lin}(\epsilon_0)$ increase as the size of the initial perturbation ϵ_0 becomes smaller. This indicates that $t_{\rm lin}$ corresponds to the crossover time at which the dynamics of a finite size perturbation depart from the linear approximation (*i.e.* the Lyapunov vectors). This crossover occurs because the tangent Lyapunov vectors describe only the behavior of strictly infinitesimal perturbations ($\epsilon_0 \to 0$). Therefore, for times $t > t_{\rm lin}(\epsilon_0)$ nonlinear corrections, due to finiteness of the initial perturbation, come into play and force the errors out of the tangent space. From then on, the linear approximation cannot describe the evolution of errors. One then expects that $t_{\rm lin}(\epsilon_0) \to \infty$ as $\epsilon_0 \to 0$.

Besides exponential growth, correlations are dynamically generated during the evolution of perturbations. Correlations contain information about the sub-leading Lyapunov exponents and thus also contribute to the perturbation size growth. The important role of correlations can be better realized after subtraction of the dominant exponential growth component given by $\epsilon(t)$. We find that a very useful indicator is given by the *reduced* perturbations $\delta r(x,t)$ that we define as

$$\delta r(x,t) = \frac{\delta u(x,t)}{\epsilon(t)}, \tag{3}$$

where the dominant exponential growth is globally removed and one is left with the effect of correlations. Statistical fluctuations of the reduced perturbations are measured by the variance $\sigma^2(t) = \langle \overline{\delta r(x,t)^2} \rangle$, where $\langle \cdots \rangle$ stands for average over realizations of the initial perturbation and the over bar is a spatial average. As we shall see below, $\sigma(t)$ gives information about the growth of perturbations due solely to correlations.

In Fig. 1 we show our numerical results for the variance of the reduced perturbations, Eq.(3). The variance $\sigma^2(t)$ grows as an exponential power law $\sigma^2(t) \sim \exp(t^{2\beta})$ for times $t < t_{\rm lin}$, *i.e.* before saturation by finiteness of the initial disturbance. A least-squared fit of $\log(\log(\sigma))$ *vs.* $\log(t)$ gives the exponent $\beta = 0.30 \pm 0.05$ (see the inset of Fig. 1). As before, this rapid growth occurs for times such that the dynamics of disturbances are well described by the Lyapunov vectors.

The magnitude and extent of spatial correlations can be measured by use of the site–site correlation function $\rho(x,t) = \langle \overline{\delta u(x_0,t) \delta u(x+x_0,t)} \rangle / \langle \overline{\delta u(x_0,t)^2} \rangle$. The magnitude of spatial correlations increases in time $\rho(x,t_1) < \rho(x,t_2)$ if $t_1 < t_2$ for times $t_1, t_2 < t_{lin}$. However, correlations become progressively smaller for times $t > t_{lin}$. This indicates that the effect of having initially finite perturbations is to introduce a characteristic time $t_{lin}(\epsilon_0)$ marking the typical time it takes for the system to depart from tangent space (with the building-up of

correlations) to truly non-linear evolution (uncorrelated errors). For times larger than t_{lin} perturbations quickly get spatially uncorrelated, as can be seen from the decay of the reduced variance in Fig. 1. Further analysis [10] shows that errors become undistinguishable from actual white noise.

Our numerical results can be explained analytically by making use of a transformation first proposed by Pikovsky and Politi for the actual Lyapunov vectors [11, 12]. We find that the dynamics of finite perturbations can also be seen as a kinetic roughening processes of the surface defined by $h(x,t) = \log|\delta u(x,t)|$. This is a very useful transformation that allows us to make use of existing results in the field of nonequilibrium surface growth. Indeed, Politi and Pikovsky [11, 12] have shown that errors in many extended systems lead to surface growth process in the universality class of KPZ [9]. Let us first consider the amplitude factor defined in Eq. (2) and show that it is related to the average surface velocity. We can write $|\delta u(x,t)| = \exp[h(x,t)]$ and thus $\epsilon(t) = \exp[(1/L)\sum_{x=1}^{x=L} h(x,t)] = \exp[\overline{h}(t)]$. We then obtain that the amplitude factor must grow as $\epsilon(t) = \epsilon_0 \exp(\lambda t)$, where λ is the largest Lyapunov exponent and corresponds to the surface velocity, in agreement with our numerical results shown in Fig. 1.

Also the time behavior of the variance of the reduced perturbations shown in Fig. 1 can be analytically related to surface scaling properties. We find that $\sigma(t)^2 = \sqrt{2\pi}\exp[2W(L,t)^2]$, where $W(L,t)$ is the surface width and depends on the system size L. This result is easily obtained by assuming a Gaussian distribution of surface heights. KPZ behavior then implies that the width scales as $W(L,t) \sim t^\beta$ for times $t < t_s(L)$ and saturates to a size dependent value, $W(L,t) \sim L^\alpha$ for $t > t_s(L)$, where β and α are the growth and roughness exponent respectively that are known to have the values $\beta = 1/3$ and $\alpha = 1/2$ for the KPZ universality class in one dimension [9]. This explains the $\exp(t^{2/3})$ scaling observed in the inset of Fig. 1. It is worth mentioning that all the numerical results presented here are obtained for system sizes such that $t_{\rm lin} \ll t_s$, so that the existence of $t_{\rm lin}$ could be clearly seen.

Dynamic scaling of bred vectors.– An important problem where finite initial errors are a concern is in weather forecasting. In this context, initial configurations that belong or are very close to the dynamical attractor are much sought after. These prepared configurations are then used as initial conditions in the atmospheric models in order to have a probabilistic forecast for a certain time window. Predictions are expected to be better when the initial conditions are closer to the dynamical attractor of the system. To achieve the goal of a maximal projection, the computer runs of the atmospheric models are started from random perturbations and BV techniques are used [7] to allow the perturbed trajectories to get closer to the chaotic attractor. BVs are defined in analogy to the operation of data reassimilation in numerical models of atmospheric evolution, in which the output of the numerical model is corrected by the observed experimental data after short periods of time $\{\tau_1, \tau_2, \tau_3..\}$. BVs are defined by multiplying each member of the ensemble by a reduction factor $\{k_1, k_2, k_3...\}$ at those times so that the amplitude factor of the perturbed solutions ϵ_0 is kept constant. Several criteria could be chosen to construct BVs. We define here what we call *continuous bred vectors* $\delta B(x,t)$ as the perturbation obtained by dividing by the amplitude factor at every time step. Since the dominant exponential growth is filtered out, BVs evolve with a constant amplitude factor by definition, but exhibit the actual spatial correlations (see [7] for further details).

We have studied the dynamics of BVs in the coupled-map lattice model given by Eq. (1). As in the case of finite perturbations we have considered a reference trajectory $u^0(x,t)$ and its corresponding ensemble of randomly perturbed trajectories $u(x,0) = u^0(x,0) + \delta u(x,0)$. But now breeding is applied so that we define the re-scaled error (the BV) $\delta\mathcal{B}(x,t) = \delta u(x,t)/\epsilon(t)$ at every time step and the perturbed trajectories are then evolved by introducing $u^0(x,t) + \epsilon_0\,\delta\mathcal{B}(x,t)$ in Eq. (1) to obtain $u(x,t+1)$. We have carried out simulations of the model for different values of the finite amplitude ϵ_0, which is the only external parameter. The implemented procedure is intended to mimic the one used in probabilistic weather forecasting [7].

The reduced perturbations $\delta r(x,t) = \epsilon_0\,\delta\mathcal{B}(x,t)$ and, in particular its variance, give a direct measure of the spatial fluctuations of the BVs. As we have shown in our previous analysis of finite perturbations, which also applies here, the variance $\sigma^2(t)$ grows with time as $\sigma^2 \sim \exp(t^{2\beta})$ until it saturates due to nonlinear terms becoming important in the equation of evolution of finite errors. The main point now is that, in contrast with the case of bare finite-size perturbations, the breeding procedure leads to a non-trivial stationary value of the statistical fluctuations of BV. More importantly, this stationary state is characterized by having space correlations, as can be seen from the finite stationary values of the variance σ^2 in Fig. 2. The time scale $\tau(\epsilon_0, L)$ characterizes the crossover to the stationary regime, where fluctuations are no longer time dependent. After that time BVs are correlated over regions of characteristic size $l(\epsilon_0, L) \sim \tau^{1/z}$, where $z = \alpha/\beta$ is the dynamic exponent. We find that numerical data of BV fluctuations can be cast in a *dynamic scaling ansatz* given by

$$\log[\sigma^2(t,\epsilon_0)] = t^{2\beta}\,\mathcal{G}(t/\tau(\epsilon_0)), \qquad (4)$$

where the scaling function $\mathcal{G}(v) \sim v^{-2\beta}$ if $v \gg 1$, and $\mathcal{G}(v) \sim$ const if $v \ll 1$. The characteristic time is found to scale as $\tau(\epsilon_0) \sim |\log(\epsilon_0)|^{1/\beta}$, as shown by collapse of the data in the inset of Fig. 2.

We can now make use of the surface growth mapping, $h(x,t) = \log|\delta\mathcal{B}(x,t)|$, to obtain some analytical understanding on the dynamic scaling behavior of BVs. Among other quantities, one can obtain the scaling law for the saturation time $\tau(\epsilon_0, L)$ as follows. Let M be the upper bound for the linear approximation to

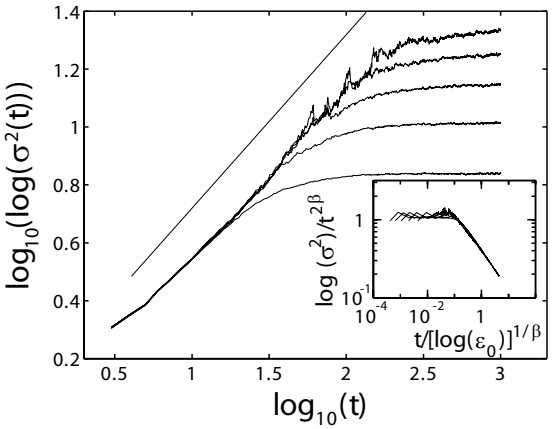

FIG. 2: Dynamic scaling of BVs for the coupled logistic maps. Main panel shows the variance $\sigma^2(t)$ *vs.* time for perturbations kept at finite amplitudes $\epsilon_0 = 10^{-3}, 10^{-4}, 10^{-5}, 10^{-6}$ and 10^{-7} (from bottom to top) by means of the breeding procedure as described in the text. The straight line has a slope 0.60 and is a guide to the eye. The inset shows a data collapse in log-log scale according to Eq. (4) with exponent $\beta = 0.28 \pm 0.05$. Results were obtained in systems of linear size $L = 1024$ and averages over 500 different initial conditions were taken.

be valid to describe the evolution of perturbations in the system. To be precise, if the error is larger than M, $|\delta u| > M$, then the time evolution of $\delta u(x,t)$ is not longer in the tangent space (infinitesimal), but finite and to be described by higher order nonlinearities. Any finite-size perturbation in the linear regime is then bounded by $\epsilon_0\, \delta\mathcal{B} < M$. This implies an upper bound in the value that the surface height can take $h_{max} \sim |\log(M/\epsilon_0)|$ and therefore a saturation time τ corresponding with the typical time for which the surface width $W(\tau) \sim h_{max}$. This leads to a characteristic time scale $\tau(\epsilon_0) \sim |\log(M/\epsilon_0)|^{1/\beta}$. This time scale together with the usual saturation time $\tau_c \sim L^z$ associated with the kinetic roughening of the surface h are the two characteristic time scales in the system. Saturation of the surface fluctuations is then controlled by the shortest of the two, $\tau(\epsilon_0, L) \sim \min\{|\log(M/\epsilon_0)|^{1/\beta}, L^z\}$. This theoretical argument agrees very well with our numerical data as can be seen in the inset of Fig. 2, where an excellent data collapse is obtained by using our theoretical expression for the saturation time $\tau \sim |\log(M/\epsilon_0)|^{1/\beta}$. For clarity of presentation all the values of ϵ_0 shown in Fig. 2 satisfy $|\log(M/\epsilon_0)|^{1/\beta} \ll L^z$ so that saturation time is governed by $|\log(M/\epsilon_0)|^{1/\beta}$. On the contrary if smaller systems are used one can see that $\tau \sim L^z$ [10].

Due to the scale–invariant dynamics of the surface $h(x,t) = \log|\delta\mathcal{B}(x,t)|$ there exists a length scale $l(\epsilon_0, L) \sim \tau(\epsilon_0, L)^{1/z}$ that corresponds to the typical extend of spatial correlations in the stationary regime. This length scale is a quantity of great importance since it can be used as an indicator of the degree of projection of the BVs into the dynamical attractor. If $l < L$ correlations are short ranged and the perturbed trajectory is only partially projected over the attractor. On the contrary, for $l > L$ BVs are spatially correlated over whole system and projection is maximal. In this case, BVs dynamics are confined to the tangent space.

Finally, we can draw some interesting conclusions for the generation and application of BVs as ensembles of initial conditions in probabilistic forecasting. For a given system size L there is a threshold $\epsilon_{th} \sim \exp(L^\alpha)$ of the fixed amplitude of BVs such that disturbances with amplitudes $\epsilon_0 < \epsilon_{th}$ propagate as infinitesimal disturbances, which dynamics are fully described by the tangent space equations (Lyapunov vectors). This in turn means that BVs are then maximally projected and correlated over whole system. In contrast, BVs with $\epsilon_0 > \epsilon_{th}$ are non infinitesimal disturbances that cannot be described by tangent space equations, but by the full nonlinear dynamics. In this case projection into the attractor is only partial and correlations have a characteristic size $l(\epsilon_0, L)$. Our results show that when using breeding techniques in probabilistic forecasting for the preparation of ensembles of initial conditions, the election of the normalization condition of the BVs is of vital importance since it introduces a previously unforeseen time/length scale related to degree of projection into the dynamical attractor.

Financial support from the Ministerio de Ciencia y Tecnología (Spain) under project BFM2000-0628-C03-02 is acknowledged.

[1] H. G. Schuster, *Deterministic Chaos, An Introduction*, VCH-Verlag, Meinheim, (1988).
[2] E. Ott, *Chaos in Dynamical Systems*, Cambridge University Press, Cambridge (1994).
[3] G. Boffetta, M. Cencini, M. Falcioni, and A. Vulpiani, Phys. Rep. **356**, 367 (2002).
[4] T. Bohr, M.H. Jensen, G. Paladin, and A. Vulpiani, *Dynamical Systems Approach to Turbulence*, Cambridge University Press, Cambridge (1998).
[5] E. Aurell, *et. al.*, Phys. Rev. Lett. **77**, 1262 (1996).
[6] D. J. Patil, *et. al.*, Phys. Rev. Lett. **86**, 5878 (2001).
[7] E. Kalnay, *Atmospheric Modeling, Data Assimilation and Predictability*, Cambridge University Press (2002).
[8] G. Francisco and P. Muruganandam, cond-mat/0212015.
[9] M. Kardar, G. Parisi, Y. C. Zhang, Phys. Rev. Lett. **56**, 889 (1986).
[10] C. Primo, M. A. Rodríguez, J. M. López, and I. Szendro (to be published).
[11] A. Pikovsky and J. Kurths, Phys. Rev. E **49**, 898 (1994).
[12] A. Pikovsky and A. Politi, Nonlinearity 11,1049 (1998).